RESEARCH LETTER

Gp66, a calcineurin family phosphatase encoded by mycobacteriophage D29, is a 2′, 3′ cyclic nucleotide phosphodiesterase that negatively regulates phage growth

Soumita Dutta, Niketa Bhawsinghka & Sujoy K. Das Gupta

Department of Microbiology, Bose Institute, Kolkata, India

Correspondence: Sujoy K. Das Gupta, Department of Microbiology, Bose Institute, P1/12 C.I.T. Scheme VIIM, Kolkata 700054, India. Tel.: 91 33 23559416; fax: 91 33 2553886; e-mail: sujoy@jcbose.ac.in

Received 22 August 2014; revised 7 October 2014; accepted 7 October 2014. Final version published online 31 October 2014.

DOI: 10.1111/1574-6968.12625

Editor: Richard Calendar

Keywords
mycobacteriophage; phosphoesterase; cyclic phosphodiesterase activity; phage growth.

Abstract

Mycobacteriophage D29 encodes a protein Gp66 which has been predicted to be a calcineurin family phosphoesterase. Phylogenetically Gp66 and related proteins mostly derived from mycobacteriophages form a distinct clade within this family. Interestingly, the presence of *gene 66* orthologs can be traced to bacteria of diverse phylogenetic lineages such as *Aquifex aeolicus*, a deep branching eubacteria and *Methanococcus jannaschii*, an archaebacteria. The promiscuous nature of *gene 66* suggests that it may have been transferred across genus barriers by horizontal gene transfer mechanisms. The biological function of members of this novel clade comprising mostly the mycobacteriophage phosphoesterases have not been elucidated so far. In this investigation, it has been demonstrated for the first time that Gp66, a member of this novel family, is a 2′, 3′ cyclic phosphodiesterase. The gene is expressed during phage infection and the net result is negative regulation of bacteriophage as well as bacterial growth.

Introduction

Calcineurin-like phosphoesterase superfamily proteins are widely distributed in bacteria and archaea. They are characterized by the presence of a conserved motif GNHD/E. Members of this family are mostly phosphohydrolases, which can hydrolyze a wide variety of phosphorylated substrates that include proteins and nucleotides (Koonin, 1994; Aravind & Koonin, 1998). Although not very common, phosphoestereases of this family have been found in bacteriophages, the best example being that belonging to bacteriophage Lambda (λ). Given that phosphoesterases can act on a variety of substrates, it is expected that synthesis of these proteins during phage infection would result in recognizable changes in the growth characteristics of the phage and perhaps the host as well. However, to date very little is known about the function of phage-encoded calcineurin family phosphoesterases including that of phage λ, which otherwise has been characterized both biochemically and structurally in detail (Barik, 1993; Voegtli *et al.*, 2000). Incidentally, calcineurin family phosphoesterases are encoded by many mycobacteriophages. Given that mycobacteriophages infect mycobacterial species, some of which such as *Mycobacterium tuberculosis* are highly pathogenic; therefore by studying the function of these phage-encoded phosphoesterases, it should be possible to derive more insight into mycobacteriophage–*Mycobacterium* interaction mechanisms. With this objective in mind, the mycobacteriophage D29 encoded protein, Gp66 which was earlier predicted to be a phosphohydrolase (Koonin, 1994) was taken up for investigation. The results indicate that unlike its λ counterpart it is not a serine–threonine protein phosphatase. However, it does possess a very specific 2′, 3′ cyclic phosphodiesterase activity. The results further demonstrate that its biological function is to act as a negative modulator of phage growth.

Materials and methods

Bacterial strains, plasmids, and phage

Escherichia coli XL1-Blue and BL21 (DE3) were used for cloning and synthesis of recombinant proteins.

FEMS MICROBIOLOGY LETTERS

Mycobacterium smegmatis mc^2155 was used for mycobacteriophage infection experiments. The expression vectors pET28a (Novagen) and pLAM12 (Addgene) were used for overexpression of recombinant genes in *E. coli* and *M. smegmatis,* respectively. Mycobacteriophage used was D29 (Ford *et al.*, 1998).

Sequence analysis by computational method

CLUSTAL W (Thompson *et al.*, 1994)-based multiple sequence alignment was performed using MEGA 5.05 (Tamura *et al.*, 2011). The protein weight matrix used was PAM (Dayhoff *et al.*, 1983), and the penalties were 10 and 1, for gap opening and gap extension, respectively. Related sequences were clustered using the neighbor-joining method (Saitou & Nei, 1987), and the final result reproduced graphically using GENEIOUS R6 (version 6.1.6) tool. Homology modeling of D29 Gp66 was performed by Swiss-Model server in the alignment mode (Arnold *et al.*, 2006) and also by I-TASSER online server. Structure-based alignments were performed using the VAST search service (http://structure.ncbi.nlm.nih.gov/Structure/VAST/vast.shtml), and these were processed for presentation using the online program ESPRIPT 3 (http://espript.ibcp.fr/ESPript/cgi-bin/ESPript.cgi).

Phage assays

Mycobacteriophage D29 infection was carried out in phage dilution medium (PDM) (0.1% tryptone, 0.2% $MgCl_2$, 0.85% NaCl) at a multiplicity of infection (MOI) of 0.1 in the presence of 2 mM $CaCl_2$. For one-step growth experiment, adsorption was carried out for 20 min at 37 °C. Following adsorption, an aliquot (2 μL) was removed and diluted to 20 mL to stop further adsorption. Aliquots (1 mL) were removed at specified intervals and centrifuged at 9300 ***g***. The phage titer in the supernatant was determined by dilution plating.

Cloning of mycobacteriophage genes in expression vectors

D29 gene*66* was amplified by PCR using primers in Supporting Information, Table S1. The PCR products were digested with either EcoRI/HindIII or NdeI/NheI and inserted into pET28a and pLAM12 vectors, respectively. Mutants of D29 gp66 were generated using a QuickChange Site-Directed Mutagenesis Kit (Stratagene) with mutagenic primers (Table S2). All gene inserts and mutations were confirmed by DNA sequencing using 3130 X Genetic Analyzer (Applied Biosystems).

Expression and purification of recombinant proteins

Recombinant pET28a constructs were transformed into *E. coli* BL21 (DE3). For the expression, one liter culture was grown at 37 °C in Luria–Bertani broth containing 0.05 mg mL^{-1} kanamycin. The culture was adjusted to 0.3 mM IPTG and shaken at 16 °C for 15 h. The cells were harvested, lysed by cell disruption equipment (Constant Systems Limited, UK) in lysis buffer [50 mM Tris-HCl (pH 8.2), 100 mM NaCl, 5 mM imidazole, 5 mM β-mercaptoethanol (β-ME), 10% glycerol, 1 mM PMSF]. The recombinant hexa-His-tagged protein was then purified from the soluble fraction by performing Ni-NTA affinity chromatography using Tris-HCl-based standard buffer system (Keppetipola & Shuman, 2007).

For the expression from pLAM12, the recombinant *M. smegmatis* cells were grown in MB7H9 medium ($OD_{600\ nm}$ = 0.2) in the presence of 0.2% succinate. Induction was achieved by adding 0.2% acetamide (Parish *et al.*, 1997). Culture aliquots were removed at different time intervals and centrifuged. Pellets were lysed, and supernatants were used either for enzyme assays or Western blot analysis.

Preparation of radiolabeled substrate for protein phosphatase assay

[γ-P^{32}] labeled MBP was prepared by phosphorylation of MBP with cAMP-dependent protein kinase A. Hundred microliters reaction mixture containing 2 μg MBP, 8 μCi [γ-P^{32}] and 1 unit kinase (NEB) was incubated at 37 °C for 1 h. Reaction was stopped by 11% TCA and stored at −20 °C. Precipitated labeled MBP was dissolved in 25 μL of Tris-HCl (pH 7.5). Phosphorylation was confirmed by performing 10% SDS-PAGE followed by autoradiography. MBP phosphorylated by this procedure results in the phosphorylation of serine–threonine residues.

Phosphoesterase assay

Cell-free extract (CFE) was prepared by disrupting cells in assay buffer followed by centrifugation (16 100 ***g***, 30 min). The soluble supernatant was then used for the assays. Reaction mixtures (200 μL) containing assay buffer [50 mM of Tris-HCl (pH-8.5), 50 mM NaCl, 1 mM $MnCl_2$, 1 mM DTT], 1 mM (or as indicated) specified substrates, and 0.1 μg of recombinant proteins or CFE were incubated for 10 min or as specified at 45 °C. The reactions were stopped by adding stop buffer [15 mM EDTA, 0.25% SDS, 5% glycerol]. Release of para-nitro phenol (pNP) was measured

spectrophotometrically at 405 nm and estimated using its molar extinction coefficient (18 450 M^{-1} cm^{-1}). Kinetic parameters were determined using GRAPHPAD-PRISM program (version 5.00 for windows).

Cyclic phosphodiesterase assay

Reaction mixtures (50 μL) containing assay buffer, 1 unit of FastAP (Fermentas), 10 mM substrate, and 0.1 μg enzyme were incubated at 45 °C for 30 min. Reactions were quenched with 1 mL of malachite green reagent (10 mL malachite green in 16% H_2SO_4 + 2.5 mL of 7.5% ammonium molybdate + 11% tween 20) and kept for 15 min. The released phosphate was determined by measuring $A_{620\ nm}$ and interpolating the value to a phosphate standard curve.

Products of cyclic phosphodiesterase activity of Gp66 were analyzed by TLC on PEI cellulose-F plate (MERCK) in a solvent containing saturated ammonium sulfate/3 M sodium acetate/isopropanol (80 : 6 : 2). Ten microliters reaction mixtures containing 5 mM of 2′, 3′ cAMP and 0.1 μg enzyme were prepared. One microliter of reaction mixture and marker (2.5 nmol of each) were spotted on TLC plate. The plate was developed for 7–8 h, visualized under UV light (254 nm), and documented using Gel-Doc system (Biorad Laboratories Inc.).

RT-PCR analysis

For RT-PCR, total RNA was isolated from *M. smegmatis* before and after D29 infection using the RNeasy Mini Kit (Qiagen). First strand cDNA was prepared from 100 ng of total RNA using Revert Aid Reverse Transcriptase (Fermentas) by random priming. Two microliters cDNA, 0.25 mM dNTPs, 0.2 pmol μL^{-1} of each primer, and 0.5 unit of Taq DNA polymerase were used for 50 μL reaction mixture. The amplified DNA was analyzed on 1.5% agarose gel in 1× TAE buffer. RT-PCR-based estimation of 16S rRNA gene levels in the samples was also performed simultaneously. All primers required for RT-PCR are listed in Table S3.

Western blot analysis of expressed protein

Mycobacterium smegmatis was infected with D29 at 0.1 MOI at 37 °C. Aliquots (1 mL) were removed at definite time intervals and harvested by centrifugation. Cell lysates were prepared by sonication and processed for Western blotting according to standardized protocols (Bhattacharya *et al.*, 2008). Antisera against Gp66 was raised in rabbit using methods described earlier (Basu *et al.*, 2002).

Results

Mycobacteriophage D29 Gp66 represents a novel clade within the calcineurin-like phosphoesterase family

In an earlier investigation, it was reported that Gp66 belongs to the calcineurin-like phosphoesterase family characterized by the presence of the motif [-GD-GNHD/E-] (Koonin, 1994). Considering that many more mycobacteriophage genomes have been sequenced (Pope *et al.*, 2014) subsequently, fresh efforts were made to investigate whether other mycobacteriophages encode similar proteins. D29 Gp66 homologs were found to be present in diverse mycobacteriophages, and these homologs formed a distinct clade within the calcineurin family (Fig. 1a). However, it was noted that λppase belongs to a different clade and so does the *M. tuberculosis* cyclic nucleotide phosphodiesterase Rv0805, another biochemically and structurally well-characterized phosphodiesterase (Shenoy *et al.*, 2007).

A structure-based search for homologous protein was then initiated. By this method, distant relative of Gp66 could be identified in diverse bacteria such as *Aquifex aeolicus*, a deep branching thermophile and *Methanococcus jannaschii*, an archaea. When the sequences corresponding to these proteins were aligned, significant conservation of secondary structure elements and important motifs were observed (Fig. 1b). Moreover, it was observed that the eubacterial and archaeal orthologs were located on a branch that is adjacent to the 'Gp66' clade confirming that all these proteins are evolutionarily related (Fig. 1a).

Phosphoesterase activity of Gp66

Considering that λppase, a distant relative of Gp66, has protein phosphatase activity, it was hypothesized that Gp66 would also be able to perform the same function. To test this possibility, the recombinant version of Gp66 protein was purified to near homogeneity (Fig. 2a) and protein dephosphorylating activities of the two proteins were compared using radiolabeled phosphorylated MBP substrate. However, the results indicate that compared to λppase, Gp66 has very little if any serine–threonine phosphoprotein hydrolase activity (Fig. 2b). To obtain further insight into its substrate specificity, phosphoesterase assays were performed using the conventional substrates: pNPP (for monoesterase activity), bis-pNPP, and TmPP (for diesterase activity) (Fig. 2c). The results show that the enzyme can use both phosphomonoester and diester as substrates. The catalytic efficiency for bis-pNPP, a diester, was found to be 10 times higher than pNPP, a monoester, although K_m values did not differ significantly

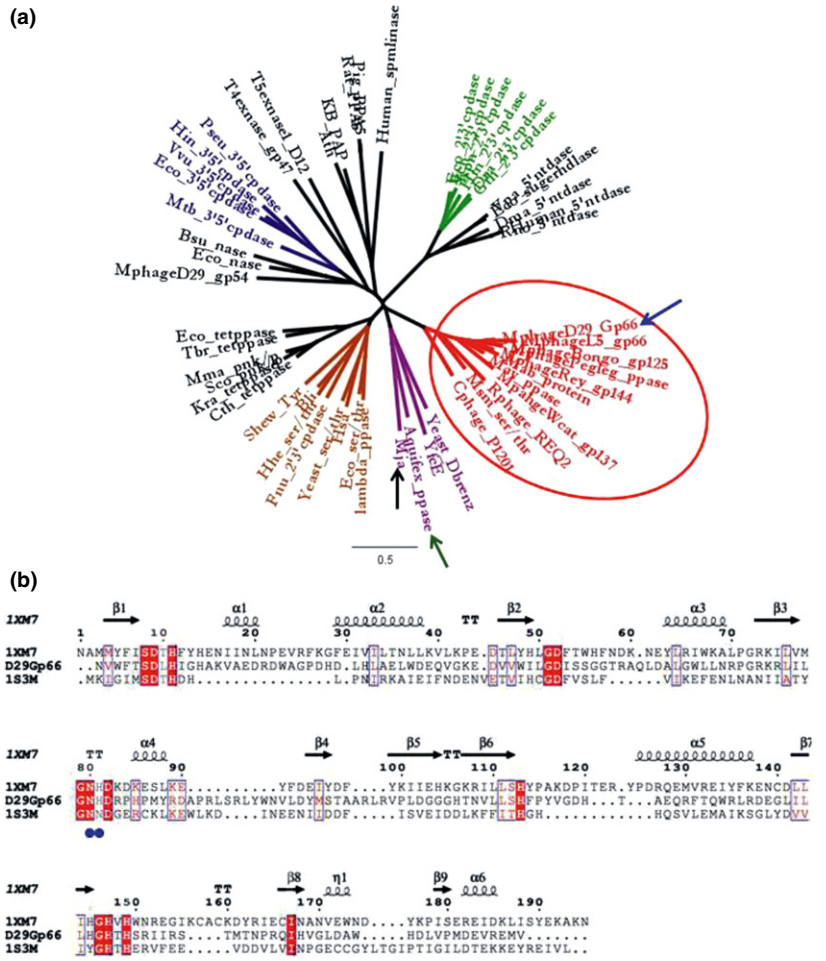

Fig. 1. Sequence alignment and phylogenetic analysis of calcineurin family phosphoesterases. (a) Phylogenetic relationship among diverse members of the calcineurin family phosphoesterase. The sequences used for the analysis, and the abbreviations used to describe the source organisms, and proteins are summarized in supplementary information (Table S4). The major branches are colored. The cluster represented by mycobacteriophage D29Gp66 is encircled. D29Gp66, *Aquifex* protein (Aquifex_ppase) and *Methanococcus* protein (Mja) are indicated by blue, green, and black arrows, respectively. The detailed alignment is shown in Fig. S1. (b) Structure-based sequence alignment of D29Gp66 with the phosphoesterases derived from *Aquifex aeolicus* (AQ665) and *Methanococcus jannaschii* (MJ0936) proteins indicated by the PDB IDs of their crystal structures 1XM7 and 1S3M, respectively. Homology modeling was initiated using the Swiss-Model and/or I-TASSER online server. The search for a possible structural homolog of D29Gp66 resulted in the identification of 1XM7 as the best possible template. VAST search using 1XM7 revealed that 1S3M is closely related to it, and therefore, the corresponding sequence was also included in the alignment. To display the conserved secondary structural elements, the VAST alignment was processed using ESPRIPT 3. Arrows and coils represent beta sheets and α helical secondary structures, respectively. Conserved sequences are blocked, and identical residues are highlighted in red. Residues for mutational analysis are shown in blue dots.

(Table 1). Overall, the results indicate that whereas the protein could function both as phosphomonoesterase as well as diesterase, the latter activity was dominant over the former.

Considering the high level of phosphodiesterase activity, it was assumed that the protein may be capable of using cyclic nucleotide phosphodiesters as substrates. To investigate this, two different substrates 2′, 3′- and 3′, 5′-cAMP were used. The results indicate that Gp66 has a strong 2′, 3′ cyclic phosphodiesterase activity and no 3′, 5′ activity (Fig. 2d, Table 1). The hydrolysable products of Gp66 were analyzed by TLC. The results show that the end products are both 2′-AMP and 3′-AMP with 2′-AMP predominating (Fig. 2e).

Mutational analysis

The GD and GNHD/E motifs of the calcineurin family proteins are highly conserved (Koonin, 1994). Mutations were performed on Gp66 to understand the role played by the various conserved amino acids. Two residues N80 and H81 (refer Fig. 1b) that are known to be present in

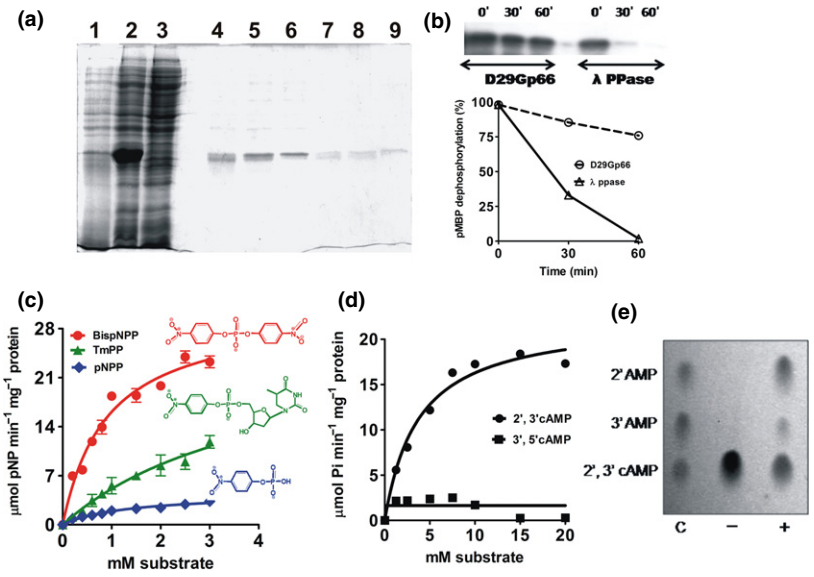

Fig. 2. Phosphoesterase activity of Gp66. (a) 12% SDS PAGE analysis of the purified hexa-histidine tagged Gp66 protein. Lanes 1, 2, 3 represent uninduced, induced, and soluble fraction, respectively, and lanes 4–9, elution fractions. (b) Protein dephosphorylation activity of D29Gp66. Protein phosphatase activity was measured using P^{32} labeled MBP as substrate. For comparison, the Lambda phage phosphatase (λppase) was included. Following incubation for indicated time periods, samples were removed and analyzed by 10% SDS-PAGE. The gel was dried and subjected to autoradiography. The image (upper panel) was scanned, and the percent dephosphorylation thus calculated represented graphically (lower panel). (c) Substrate saturation kinetics using increasing concentrations of the various substrates, the chemical structures of which are indicated in matching colors. Each data point represents the average of three estimations ± SD. (d) Cyclic phosphodiesterase activity of Gp66 protein. Specific activities of the enzyme were determined at increasing concentration of either 2′, 3′- or 3′, 5′ cyclic AMP. Curve fitting was performed using the Michaelis–Menten equation to obtain the K_m and V_{max}. (e) TLC analysis of products obtained after hydrolysis of the cyclic phosphodiester substrate 2′, 3′ cyclic AMP. For comparison, a mixture of 2′, 3′ cyclic AMP and its two possible hydrolysis products 2′- and 3′-AMPs were loaded (lane c). Experiments were carried out either in the absence (–) or presence of the enzyme (+).

Table 1. Phosphoesterase activity of different phage enzymes

Protein	Substrate	K_m (mM)	V_{max} (μmol min^{-1} mg^{-1})	K_{cat} (s^{-1})	K_{cat}/K_m (s^{-1} M^{-1})
Gp66	pNPP	1.33 ± 0.25	4.49 ± 0.39	1.73 ± 0.31	1.3×10^3
	bis-pNPP	0.91 ± 0.17	30.79 ± 2.21	12.83 ± 0.94	1.4×10^4
	TmPP	5.05 ± 0.51	29.0 ± 1.61	14.06 ± 2.01	2.8×10^3
	2′, 3′-cAMP	3.74 ± 0.75	22.39 ± 1.43	8.17 ± 1.8	2.18×10^3
	3′, 5′-cAMP	–	–	–	–
66N80A	bis-pNPP	2.22 ± 0.28	1.18 ± 0.53	0.98 ± 0.04	0.2×10^3
66H81A	bis-pNPP	23.46 ± 4.02	63.74 ± 9.4	46.8 ± 7.83	1.14×10^3

the active center were targeted (Zhang *et al.*, 1996). The phosphodiesterase activity of the mutants N80A and H81A was then analyzed using bis-pNPP as substrate. The results indicate that while both mutations adversely affected activity, the effect in case of N80A was significantly more as compared to H81A (Fig. 3a). Substrate saturation experiments revealed that in case of N80A (Fig. 3b), the K_m remained almost the same but V_{max} was reduced substantially (Table 1), whereas in H81A (Fig. 3c), the major effect was on K_m rather than V_{max} (Table 1). In the case of H81A mutant, saturation could not be achieved even at the maximum possible concentration of substrate. This observation indicates that H81A has considerably lower affinity (higher K_m) for bis-pNPP as compared to either the wild type (WT) or the mutant N80A. Thus, H81 residue determines substrate affinity, whereas N80 contributes to the hydrolysis process apparently by chelating hydrolytically active metal ions (Shenoy *et al.*, 2007).

Expression of *gene 66* in phage-infected cells

Expression of the gene *gp66* in phage-infected *M. smegmatis* was investigated first by performing

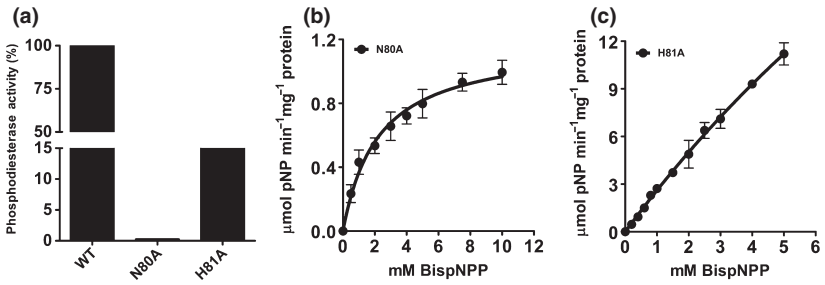

Fig. 3. Mutational analysis of Gp66. (a) Comparative analysis of phosphodiesterase activity of Gp66 either WT or the mutants as indicated. (b and c) Effect of N80A and H81A mutations (b and c, respectively) on K_m and V_{max}. Specific activity (mean ± SD) was determined for mutants at increasing substrate concentrations. Curve fitting was performed using Michaelis–Menten equation followed by determination of K_m and V_{max}.

RT-PCR (Fig. 4a) and then by Western blot analysis (Fig. 4b). Both experiments revealed that the gene is expressed in *M. smegmatis* following D29 infection after about 30 min. In the Western blot (Fig. 4b), an additional band corresponding to a protein having higher M_w is visible. However, the same band is also present in the uninfected control, indicating that it represents a cross-reactive protein derived from the host.

Considering that the latent phase of mycobacteriophage is about 90 min (Giri *et al.*, 2009), the timing of *gene 66* expression may be described as middle–early. An increase in 2′, 3′-cAMP hydrolyzing activity was observed in infected cells at about 120 min which approximately coincides with the late phase of phage growth. In case of uninfected cells, a basal level of 2′, 3′-cAMP phosphodiesterase activity was observed, which increased marginally with the growth of the uninfected cells; however, no discrete peak was observed at any stage (Fig. 4c). Hence, Gp66 probably has some role to play in the middle or late phase of D29 growth.

The N80A mutant has a dominant negative effect on Gp66 activity *in vivo*

The genes for Gp66 (WT) and the corresponding null N80A mutant were cloned in the inducible vector pLAM12. Following introduction of recombinant plasmids into *M. smegmatis* host cells, gene expression was induced by addition of acetamide. At timed intervals, cells were lysed and phosphatase activities in the extracts were assessed using bis-pNPP as substrate. The results show that in case of WT, the activity increased in a time-dependent manner as expected and saturated after 180 min of growth under inducible conditions (Fig. 5a, blue trace). In case of the mutant, however, no significant activity was observed (Fig. 5b). The lack of phosphatase activity in host cells expressing mutant gene was not due to inadequate synthesis of the protein. This is evident from Western blot analysis which shows that there is no

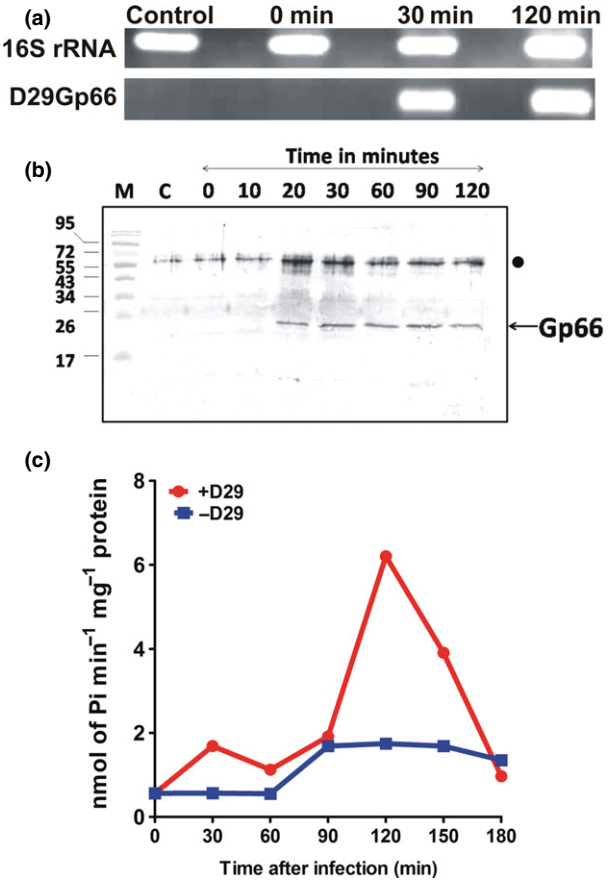

Fig. 4. Expression of Gp66 in phage-infected *Mycobacterium smegmatis*. Host cells were infected with mycobacteriophage. Samples were taken out from uninfected cells (control) and either immediately after addition of phage (0 min) or at the indicated time points and analyzed either by RT-PCR (a) or Western blotting with Gp66 antisera (b) or enzyme assays using 2′, 3′-cAMP (c). In the case of (c), the uninfected cells were also monitored for activity. The activities in the infected and uninfected cells are indicated by red and blue traces, respectively. In the Western blot, the band corresponding to Gp66 is indicated. The dot indicates an additional band, which apparently represents a cross-reactive host protein. The sizes (kDa) of the protein markers used are indicated on the left.

major difference in the amount of protein synthesized between the cells expressing WT (Fig. 5c) and mutant genes (Fig. 5d). An aliquot of the cells expressing *gene 66* was removed after 180 min time point and infected with phage (Fig. 5a, denoted by arrow). The time-dependent change in phosphatase activity of phage-infected cells was then assessed (red traces). The results indicated that in phage-infected cells, an increase in activity was observed over and above the basal level (Fig. 5a). The increased activity level, however, declined in a manner similar to

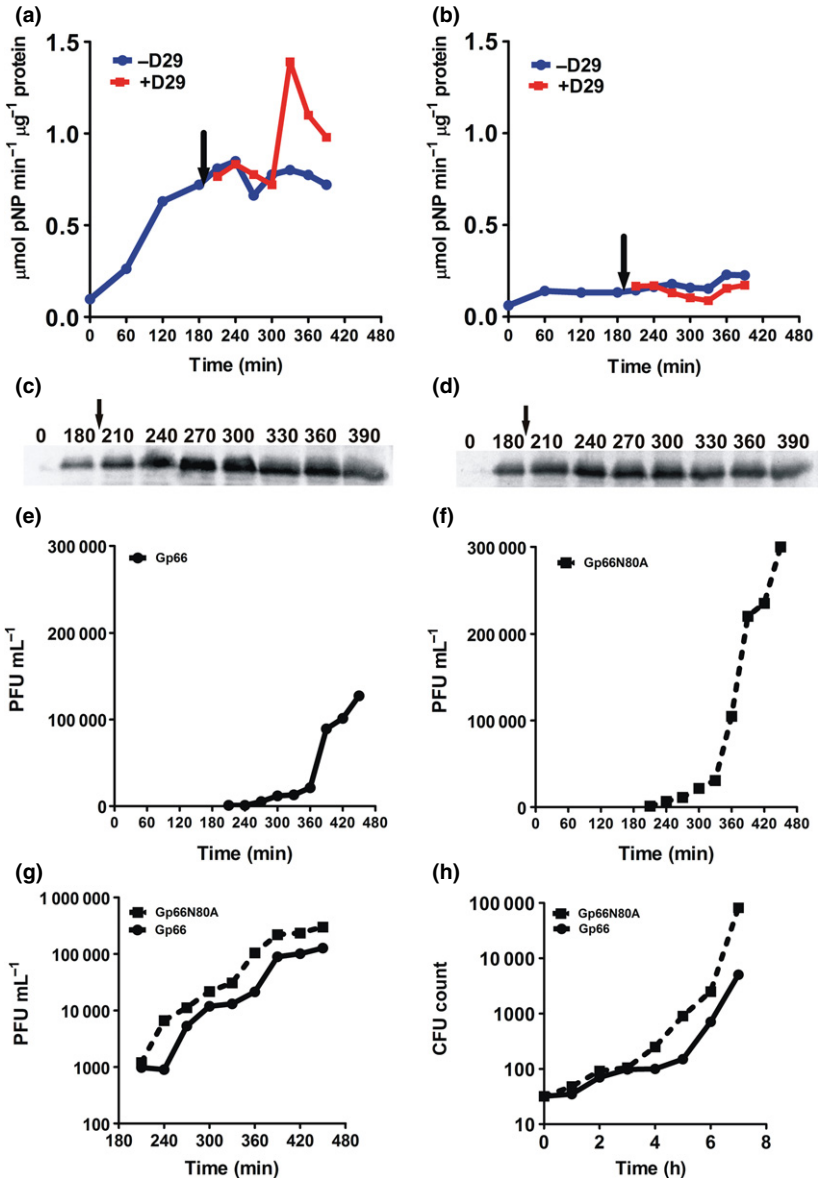

Fig. 5. The effect of *gene 66* expression on phage growth. Phosphatase activity of *Mycobacterium smegmatis* cells expressing the gene encoding Gp66 either WT (a) or the mutant (b) from pLAM12-based vectors following induction with acetamide with (+) or without (−) D29 infection as indicated. The phage was added after 180 min time point as indicated by the down arrow. Phosphatase activity was determined by estimating the color produced upon release of pNP from bis-pNPP spectrophotometrically and expressed as µmoles of pNP released per min per mg protein. (c and d) Western Blot analysis for detecting the presence of Gp66 in phage-infected cells expressing either the WT or mutant version of *gene 66*, (c and d), respectively. The 0 min time point represents the uninduced state. Samples were recovered from time to time and analyzed. The arrow indicates the time at which phage was added. (e and f) One-step growth kinetics of phages infecting *Mycobacterium smegmatis* synthesizing either Gp66 (e) or the N80A mutant (f). (g) Combined logarithmic plot of the data presented in (e and f). (h) Effect of Gp66 expression on host cell growth. Viable counts were determined at the indicated time points. In (e–h) solid and dotted lines represent growth kinetics performed using Gp66 or Gp66N80A synthesizing cells, respectively.

that observed when phage-infected nonrecombinant host cells were examined (refer to Fig. 4c). Thus even though, the basal level of Gp66 activity was high in the recombinant cells under inducible condition, expression of the phage allele could be detected over and above the background (Fig. 5a). When the same experiment was performed in cells expressing mutant protein, the observed spike in the expression of the phage allele could not be detected, even though the background phosphatase activity in these cells was low (Fig. 5b). This result indicates that not only does the mutant have no activity of its own, it has a dominant negative effect on the activity of the product synthesized from the WT allele.

Gp66 is a negative modulator of phage and host cell growth

The ability of the N80A mutant to suppress Gp66 activity was then used for investigating the function of Gp66. It was observed that the phage growth in cells expressing the WT gene was almost three times less as compared to those expressing the mutant (Fig. 5e compared to 5f). To understand better the effect of ectopic expression of *gene 66* on phage growth, a logarithmic plot was carried out using data derived from the linear plots. The results show that the basic difference is that there is a delay (*c.* 40 min) in the onset of the lytic phase in *gene 66* expressing WT cells, relative to those expressing the mutant (Fig. 5g). The results therefore indicate that Gp66 plays an important role in negatively regulating growth cycle of the phage. The negative effect is possibly mediated through a similar effect on the host itself. This is evident from the observation that in cells expressing *gene 66*, growth is retarded as compared to those expressing the mutant (Fig. 5h). The time point (2–4 h) at which the retarded growth commences coincides approximately with that at which Gp66 activity reaches maximal levels following induction of expression (Fig. 5a). The results therefore demonstrate that Gp66 negatively modulates phage as well as host cell growth, possibly by dephosphorylating some important phosphorylated component derived either from the host or the phage or both.

Discussion

In this study, the function of the protein encoded by *gene 66* of mycobacteriophage D29 has been investigated. The mycobacteriophages that possess *gene 66* homologs can be found not only in members of A2 family (Hatfull *et al.*, 2010) to which D29 belongs, but also several others outside the family such as the singleton Wildcat and the cluster M phages, Bongo, Pegleg, and Rey (Pope *et al.*, 2014). Hence, it appears that this gene has been transferred from one mycobacteriophage family to another through illegitimate recombination mechanisms on more than one occasion. The phylogenetic analysis further revealed that orthologs of D29 Gp66 are present in the deep branching eubacteria *A. aeolicus* and the archaebacteria *M. jannaschii*. It is possible that orthologs of *gene 66* were transferred horizontally from one domain to another at some stage in evolution through the mediation of an ancient virus related to A2 cluster mycobacteriophages.

Gp66 was found to be highly active on cyclic nucleotide monophosphates particularly 2′, 3′-cAMP. The 2′, 3′ cyclic phosphodiester is generally formed during RNA metabolism including tRNA repair and splicing (Tanaka *et al.*, 2011). Repairing these products require that these cyclic products are hydrolyzed to release free 3′-OH end that can be ligated to phosphorylated 5′-ends. Phage T4 PNK/P possesses a phosphatase domain which does this function (Das & Shuman, 2013). It is possible that Gp66 may have some role to play in RNA degradation and repair.

The observation that Gp66 is actively synthesized during the middle phase of phage growth suggests that it has an important role to play in phage development. A 2′, 3′ cyclic phosphodiesterase activity was found to peak approximately in the late stages of growth in phage-infected cells. It is likely that the increased activity in phage-infected cells is due to the phage protein, although the possible activation of a host enzyme cannot be ruled out.

Site directed mutagenesis of mycobacteriophages is technically difficult. A recombineering-based method developed for mycobacteriophages did not lead to the desired results. For reasons unknown, such methods do not appear to work efficiently in case of D29 and related phages (Savinov *et al.*, 2012). In this context, the ability of Gp66 N80A mutant to exert a dominant negative effect on the activity of WT protein *in vivo*, allowed us to examine the possible role of Gp66. Mutant proteins can exert dominant negative effects on their WT counterparts, by a variety of mechanisms (Herskowitz, 1987) which includes the formation of inactive multimers and competitive inhibition. Size-exclusion chromatography revealed that Gp66 is monomeric (data not shown). Hence, inactivation through the formation of mixed aggregates is probably not the mechanism. Preliminary investigations have revealed a possible competitive type mechanism of inhibition, in which the mutant competes for the substrate without hydrolyzing it. As the K_m of N80A mutant and WT are similar, such an explanation seems valid. These experiments were, however, performed *in vitro. In vivo,* the mechanism could be far more complex.

Inhibition of Gp66 activity was found to result in increased phage proliferation indicating that the protein

negatively regulates D29 growth. The presence of Gp66 was also found to have a transient negative effect on the growth of the host as well. Thus, it appears that when Gp66 activity reaches its peak, growth of the host and phage halts, though transiently. As Gp66 activity declines, growth of host and phage resumes. Exactly, why the phage should possess a negative regulatory circuit is not clear at present. It is possible that this negative circuit delays the lytic cycle to facilitate lysogeny. The mechanism could be somewhat similar to the temporal regulation of lytic-lysogeny decision observed in the case of phage λ (Oppenheim *et al.*, 2005).

Acknowledgements

We thank Dr R. McNerney for D29 phage. We are grateful to P. Halder for his technical assistance. S.D. acknowledges CSIR, Govt. of India and N.B. acknowledges UGC, Govt. of India for their financial assistance.

References

Aravind L & Koonin EV (1998) Phosphoesterase domains associated with DNA polymerases of diverse origins. *Nucleic Acids Res* **26**: 3746–3752.

Arnold K, Bordoli L, Kopp J & Schwede T (2006) The SWISS-MODEL workspace: a web-based environment for protein structure homology modelling. *Bioinformatics* **22**: 195–201.

Barik S (1993) Expression and biochemical properties of a protein serine/threonine phosphatase encoded by bacteriophage lambda. *P Natl Acad Sci USA* **90**: 10633–10637.

Basu A, Chawla-Sarkar M, Chakrabarti S & Das Gupta SK (2002) Origin binding activity of the Mycobacterial plasmid pAL5000 replication protein RepB is stimulated through interactions with host factors and coupled expression of repA. *J Bacteriol* **184**: 2204–2214.

Bhattacharya B, Giri N, Mitra M & Gupta SK (2008) Cloning, characterization and expression analysis of nucleotide metabolism-related genes of mycobacteriophage L5. *FEMS Microbiol Lett* **280**: 64–72.

Das U & Shuman S (2013) Mechanism of RNA 2′,3′-cyclic phosphate end healing by T4 polynucleotide kinase-phosphatase. *Nucleic Acids Res* **41**: 355–365.

Dayhoff MO, Barker WC & Hunt LT (1983) Establishing homologies in protein sequences. *Methods Enzymol* **91**: 524–545.

Ford ME, Sarkis GJ, Belanger AE, Hendrix RW & Hatfull GF (1998) Genome structure of mycobacteriophage D29: implications for phage evolution. *J Mol Biol* **279**: 143–164.

Giri N, Bhowmik P, Bhattacharya B, Mitra M & Das Gupta SK (2009) The mycobacteriophage D29 gene 65 encodes an early-expressed protein that functions as a structure-specific nuclease. *J Bacteriol* **191**: 959–967.

Hatfull GF, Jacobs-Sera D, Lawrence JG *et al.* (2010) Comparative genomic analysis of 60 Mycobacteriophage genomes: genome clustering, gene acquisition, and gene size. *J Mol Biol* **397**: 119–143.

Herskowitz I (1987) Functional inactivation of genes by dominant negative mutations. *Nature* **329**: 219–222.

Keppetipola N & Shuman S (2007) Characterization of the 2′,3′ cyclic phosphodiesterase activities of Clostridium thermocellum polynucleotide kinase-phosphatase and bacteriophage lambda phosphatase. *Nucleic Acids Res* **35**: 7721–7732.

Koonin EV (1994) Conserved sequence pattern in a wide variety of phosphoesterases. *Protein Sci* **3**: 356–358.

Oppenheim AB, Kobiler O, Stavans J, Court DL & Adhya S (2005) Switches in bacteriophage lambda development. *Annu Rev Genet* **39**: 409–429.

Parish T, Mahenthiralingam E, Draper P, Davis EO & Colston MJ (1997) Regulation of the inducible acetamidase gene of *Mycobacterium smegmatis*. *Microbiology* **143**(Pt 7): 2267–2276.

Pope WH, Anders KR, Baird M *et al.* (2014) Cluster M Mycobacteriophages Bongo, PegLeg, and Rey with unusually large repertoires of tRNA isotypes. *J Virol* **88**: 2461–2480.

Saitou N & Nei M (1987) The neighbor-joining method: a new method for reconstructing phylogenetic trees. *Mol Biol Evol* **4**: 406–425.

Savinov A, Pan J, Ghosh P & Hatfull GF (2012) The Bxb1 gp47 recombination directionality factor is required not only for prophage excision, but also for phage DNA replication. *Gene* **495**: 42–48.

Shenoy AR, Capuder M, Draskovic P, Lamba D, Visweswariah SS & Podobnik M (2007) Structural and biochemical analysis of the Rv0805 cyclic nucleotide phosphodiesterase from *Mycobacterium tuberculosis*. *J Mol Biol* **365**: 211–225.

Tamura K, Peterson D, Peterson N, Stecher G, Nei M & Kumar S (2011) MEGA5: molecular evolutionary genetics analysis using maximum likelihood, evolutionary distance, and maximum parsimony methods. *Mol Biol Evol* **28**: 2731–2739.

Tanaka N, Chakravarty AK, Maughan B & Shuman S (2011) Novel mechanism of RNA repair by RtcB via sequential 2′,3′-cyclic phosphodiesterase and 3′-Phosphate/5′-hydroxyl ligation reactions. *J Biol Chem* **286**: 43134–43143.

Thompson JD, Higgins DG & Gibson TJ (1994) CLUSTAL W: improving the sensitivity of progressive multiple sequence alignment through sequence weighting, position-specific gap penalties and weight matrix choice. *Nucleic Acids Res* **22**: 4673–4680.

Voegtli WC, White DJ, Reiter NJ, Rusnak F & Rosenzweig AC (2000) Structure of the bacteriophage lambda Ser/Thr protein phosphatase with sulfate ion bound in two coordination modes. *Biochemistry* **39**: 15365–15374.

Zhang J, Zhang Z, Brew K & Lee EY (1996) Mutational analysis of the catalytic subunit of muscle protein phosphatase-1. *Biochemistry* **35**: 6276–6282.

Supporting Information

Additional Supporting Information may be found in the online version of this article:

Table S1. List of primers for cloning of mycobacteriophage protein.

Table S2. List of primers for constructing D29Gp66 mutant proteins.

Table S3. List of primers for RT-PCR.

Table S4. Detail description of the taxa used in phylogenetic analysis.

Fig. S1. Sequence alignment and constructed phylogenetic tree of phosphoesterase proteins.